

# Detection of Hydrogen Leakage in a Composite Sandwich Structure at Cryogenic Temperature

H. Kevin Rivers\* and Joseph G. Sikora†

*NASA Langley Research Center, Hampton, Virginia 23681*

and

Sankara N. Sankaran‡

*Lockheed Martin Space Operations, Hampton, Virginia 23681*

Hydrogen tanks made of polymer-matrix composite material have been proposed as an enabling technology for reducing the weight of reusable launch vehicles and increasing their payload. A key development issue for these lightweight structures is the leakage of hydrogen through the composite material, which is generally a function of the tank material, manufacturing method, mechanical load, any internal damage states in the material, and the temperatures at which the tank must operate. A method for measuring leakage through a geometrically complex structure at cryogenic temperatures and under mechanical load that has been developed, calibrated, and used to measure helium and hydrogen leakage through the X-33 liquid hydrogen tank structure is presented. In particular, results from the calibration tests are presented that indicate that the measurement errors are less than 10% for leak rates ranging from 0.3 to 200 cm<sup>3</sup>/min at standard atmospheric conditions. In addition, both hydrogen and helium leak tests that were performed on two specimens taken from a discarded segment of the X-33 tank structure and results are compared. For both the hydrogen and helium tests leak rates varied with the applied mechanical load. The level of hydrogen leakage is shown to be significantly higher than the helium leakage and to exceed the acceptable leak rate for a vehicle like the X-33 liquid hydrogen tank by an order of magnitude.

## Introduction

RECENT research on reusable launch vehicles has focused on reducing the cost of delivering payloads to orbit.<sup>1</sup> An important aspect of reducing this cost is the reduction of launch-vehicle structural weight. Liquid hydrogen (LH<sub>2</sub>) tanks can be the largest structural component of a launch vehicle, and so the design of lightweight hydrogen tanks can have a large influence on reducing the cost of space access. Polymer-matrix composite (PMC) hydrogen tanks have been proposed by Dixon et al.<sup>2</sup> as an enabling technology for reducing the weight of reusable launch vehicles. Because of this potential benefit, NASA and Lockheed Martin undertook the development of the X-33 reusable launch vehicle, which incorporates two PMC LH<sub>2</sub> tanks (see Fig. 1).

A significant development issue for these composite structures is the prevention of hydrogen leakage through the tank wall. Hydrogen is difficult to contain because of its small molecular size, and containment of hydrogen is critical because of its chemical reactivity. Concentrations of hydrogen in air above 4% by volume are flammable, and hydrogen can detonate in air when concentrations reach 18.3% by volume.<sup>3</sup> There are many places in a reusable launch vehicle that can be filled with hydrogen, for example, spaces between the hydrogen tank and aeroshell and between the LH<sub>2</sub> tanks

and the liquid oxygen tank (intertank volumes), to name a few. Because the presence of these open cavities is dependent on a particular launch-vehicle concept, the acceptable hydrogen leak rate also varies with the vehicle-concept definition. For example, for the National Aerospace Plane and the single-stage-to-orbit vehicles<sup>4</sup> acceptable leak rates for the hydrogen tanks were based on the total amount of leakage expected through fittings and valves, which was calculated to range from 10<sup>-4</sup> to 10<sup>-3</sup> scc/s-in.<sup>2</sup>.

The Lockheed Martin X-33 vehicle design incorporates two PMC LH<sub>2</sub> tanks, shown schematically in Fig. 1. To more effectively fill the lifting-body shaped tanks, the barrel section of each tank was fabricated by joining four conical sections called "lobes." This approach yielded quad-lobed tanks, with each having honeycomb-core sandwich wall construction. Both facesheets of the sandwich were graphite-epoxy (IM7/977-2) material, and the core material was a 3-pcf, unvented, aramid-phenolic honeycomb.

During preflight proof testing, the first X-33 LH<sub>2</sub> tank failed when the pressure increased in the core of the sandwich tank wall causing the facesheets to disbond and separate from the core material, as shown in Fig. 2. An investigation team determined the most probable cause of the failure to be a combination of microcracking of the inner facesheet with subsequent gaseous hydrogen infiltration, cryopumping of the exterior nitrogen purge gas, reduced bondline strength and toughness, and manufacturing flaws and defects.<sup>5</sup>

Many factors contribute to the leakage of gases through materials. For example, porosity, manufacturing flaws, and internal damage each contribute to the permeability of a material. In PMC materials the greatest contributor to leakage is believed to be microcracks that form leak paths that allow liquids or gases to pass through the material.<sup>5,6</sup> In Ref. 5 a ply-level stress analysis was performed for the X-33 LH<sub>2</sub>-tank inner facesheet that used Classical Lamination Theory.<sup>7</sup> The thermal residual stresses in the plies caused by cooldown from the stress-free temperature were computed and compared with transverse ply strength values for the IM7/977-2 material. The results suggest that microcracking probably occurred. It was also noted in Ref. 5 that microcracking is likely to occur in most PMC materials at -423°F (LH<sub>2</sub> temperature) because of large thermal residual stresses, large mechanical stresses, and low transverse matrix strength. Not only do the thermal and mechanical stresses cause microcracking in PMC materials, but when microcracks already exist within a laminate the combination of these

Received 14 February 2001; presented as Paper 2001-1218 at the AIAA/ASME/ASCE/AHS/ASC 42nd Structures, Structural Dynamics, and Materials Conference, Seattle, WA, 16–19 April 2001; revision received 2 January 2002; accepted for publication 23 January 2002. Copyright © 2002 by the American Institute of Aeronautics and Astronautics, Inc. No copyright is asserted in the United States under Title 17, U.S. Code. The U.S. Government has a royalty-free license to exercise all rights under the copyright claimed herein for Governmental purposes. All other rights are reserved by the copyright owner. Copies of this paper may be made for personal or internal use, on condition that the copier pay the \$10.00 per-copy fee to the Copyright Clearance Center, Inc., 222 Rosewood Drive, Danvers, MA 01923; include the code 0022-4650/02 \$10.00 in correspondence with the CCC.

\*Aerospace Engineer, Metals and Thermal Structures Branch, Structures and Materials Competency, 6 E. Reid Street.

†Aerospace Engineer, Instrumentation Systems Development Branch, Aerodynamics, Aerothermodynamics and Acoustics Competency.

‡Senior Scientist and Metals Group Leader. Member AIAA.

stresses can cause the microcracks to grow and increase the rate of leakage through the material. For this reason, leakage should be studied for the full spectrum of operational mechanical and thermal loads while the material is at the operational temperature and under mechanical load.

Typically, permeability tests are performed on small coupon specimens without accounting for mechanical or thermal loads, using helium or hydrogen as the test gas.<sup>8</sup> These tests are useful for screening materials and fabrication processes, but they do not adequately address the important issue of determining the in situ rate of hydrogen leakage in built-up structural components exposed to combined thermal and mechanical loads. The present study was motivated by the need to measure hydrogen leakage through actual X-33 tank structure that was subjected to mechanical load at the operational cryogenic temperature. Another issue that must be considered when designing a leak measurement system is the expected level of leakage through the structure. During fill/drain tests of the X-33 tank, the pressure inside the sandwich structure rose rapidly after being exposed to hydrogen,<sup>5</sup> indicating levels of leakage higher than typical permeation rates, which are usually less than  $10^{-4}$  scc/s-in.<sup>2</sup>. For this reason, a measurement system was designed to measure microleaks or leaks that range from  $10^{-4}$  scc/s-in.<sup>2</sup> to

$10^{-2}$  scc/s-in.<sup>2</sup>. There is no known leak measurement system capable of measuring leaks (of these magnitudes) through complex-shaped structures that are mechanically loaded at operational, cryogenic temperature.

The objective of the present study was to quantify accurately the in-situ leakage of helium or hydrogen through complex, built-up, mechanically loaded structures that have been cooled to cryogenic (liquid-hydrogen) temperatures. To accomplish this objective, a novel leak detection system was developed at the NASA Langley Research Center. The objective of the present paper is to describe this leak detection system and illustrate its application. Toward that objective, the test specimens, mechanical loading setup, and instrumentation are described. Next, the tests that were conducted to calibrate the system are described. Subsequent tests that were conducted and the results that were obtained are then presented. Last, an in-depth discussion of the test results and their implications is presented.

### Flexible Microleak Detection System

The flexible microleak detection system (FMLDS) is shown schematically in Fig. 3. The system consists of a flexible aluminized Mylar™ vacuum membrane, sealed to a test specimen with a vacuum seal material (Fig. 4), and a microleak collection and measurement system. When tests were performed at cryogenic temperatures, compressed foam was placed beneath the test panel and used to maintain a slight positive pressure on the seal. The seal was kept above 0°F to maintain an acceptable vacuum seal. Heated ethylene glycol was circulated through a 0.125-in.-diam copper tube embedded in the center of the seal. Gases that leaked through the test specimen were captured in a space maintained by a scrim cloth under the vacuum membrane and were vented through a 0.0625-in.-diam stainless-steel capillary tube to an evacuated control volume. The capillary tube was connected to the control volume through 0.25-in. stainless-steel tubing. Changes in pressure and temperature in the evacuated control volume were measured and then used to calculate a rate of mass flow by using the ideal-gas law.<sup>9</sup> A mass spectrometer, used to determine the gas species that leaked into the system, verified that the leak being measured was not from a source other than the test panel. In the event of very low leak rates (less than  $10^{-4}$  scc/s-in.<sup>2</sup>), the mass spectrometer was used to determine the rate of permeation.

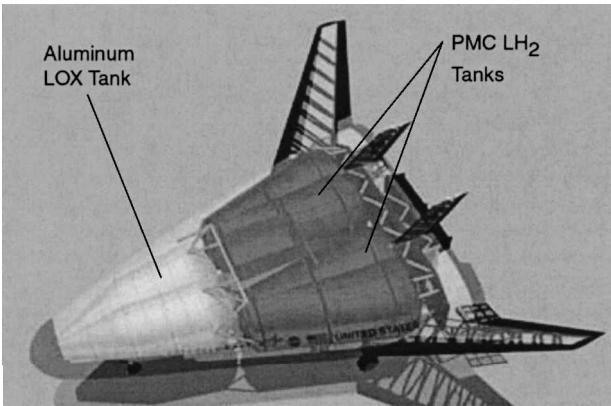


Fig. 1 X-33 structural arrangement showing quad-lobed liquid hydrogen tanks and dual-lobed liquid-oxygen tank.

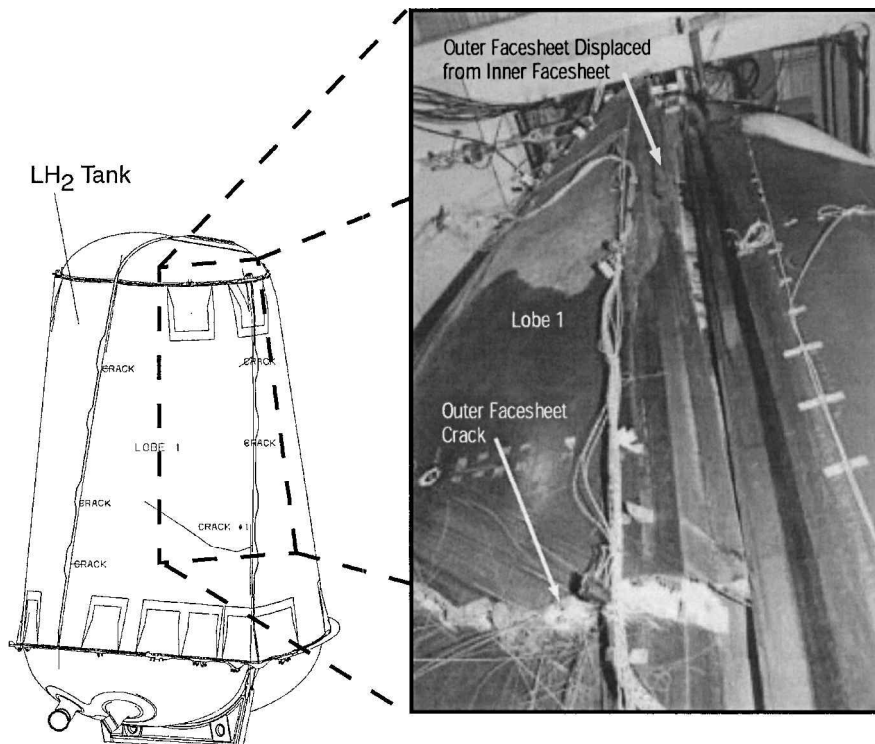


Fig. 2 Schematic and photograph of the failed X-33 LH<sub>2</sub> tank indicating cracks and outer facesheet disbonds.

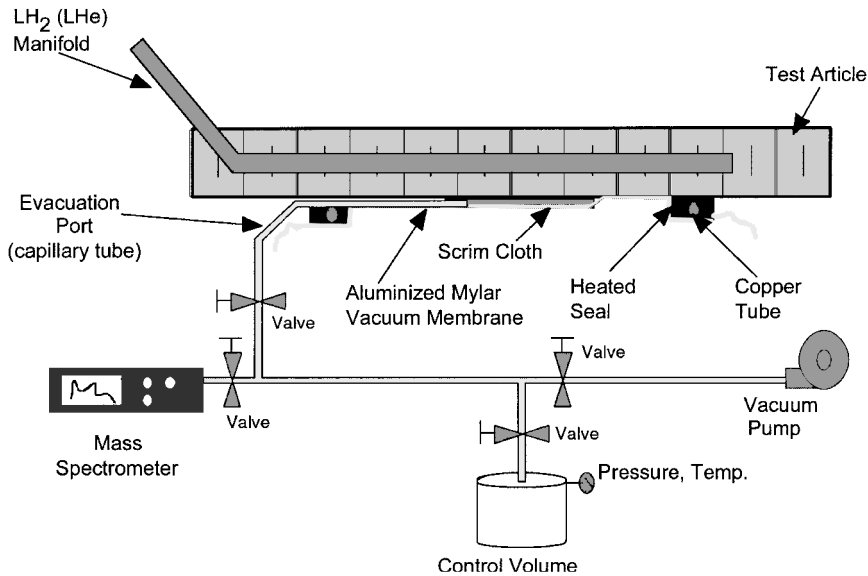


Fig. 3 Schematic of the Flexible Micro-Leak Detection System.

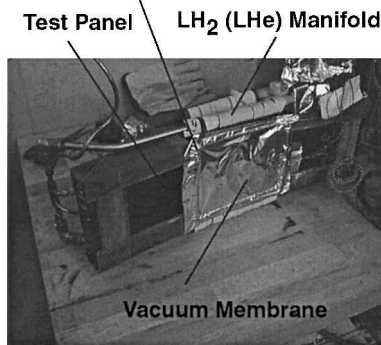
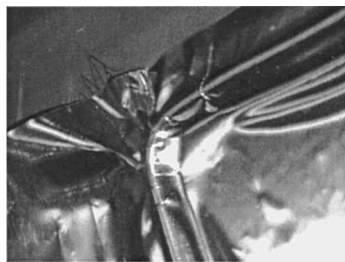


Fig. 4 Test panel with vacuum membrane and cryo manifold installed.

### Test Articles and Instrumentation

Two test articles were evaluated for both liquid helium (LHe) and  $\text{LH}_2$  leakage. Both test specimens were cut from a conical section (or lobe) of the X-33  $\text{LH}_2$  tank that had been replaced because of manufacturing flaws. Both test specimens were nominally 24 in. long and 7 in. wide (Fig. 5). The specimens were doubly curved with a radius of 65 in. in the hoop direction (as shown in Fig. 5) and 156 in. in the transverse direction (also indicated in Fig. 5).

The specimens were graphite-epoxy (IM7/977-2) sandwich construction consisting of an inner facesheet of cross-ply tape with a stacking sequence of  $[\pm 45/90_3/\pm 45/0_{1.5}]_s$  and an outer facesheet with a stacking sequence of  $[\pm 65/0/65/90_{0.5}]_s$ . The 0- and 90-deg-ply orientations correspond to the hoop and transverse directions in the test article, respectively. The honeycomb core material was 1 in. thick.

In these tests an in-plane tensile load was introduced (in the hoop direction) to the inner facesheet by loading the specimen in four-point bending (Fig. 6). Because the shear strength of the core was very low, fiberglass reinforcements were added in the load introduction region (Fig. 7). Because the outer facesheet was thinner than

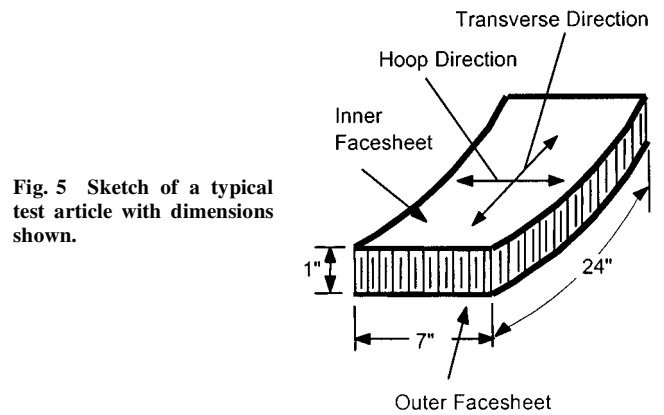


Fig. 5 Sketch of a typical test article with dimensions shown.

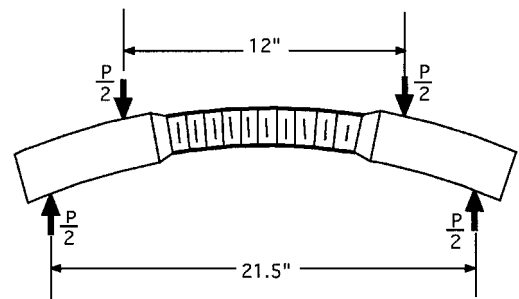
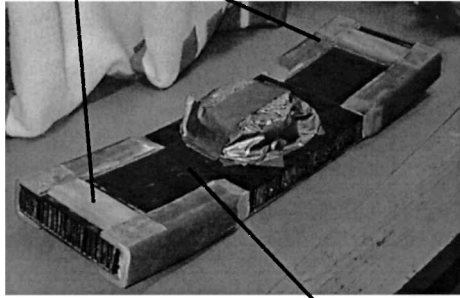


Fig. 6 Schematic indicating how in-plane tensile load was introduced into the inner facesheet through four-point bending.

the inner facesheet, a layer of fiberglass material was bonded to it to prevent its failure. Both of these reinforcements are illustrated in the photograph shown in Fig. 8. The specimen's temperature was maintained at  $-423^\circ\text{F}$ , and the source for leak gas was provided by introducing cryogenic fluids into the core of the sandwich through a stainless-steel manifold. Ten 0.25-in.-diam holes were machined in the core at the center of the panel with 0.5-in. spacing to accommodate the manifold. Under four-point bending the shear in this region of the core was negligible. Holes, 0.0625 in. in diameter, were then drilled through each cell of the core to ensure that the cryogen entered all of the cells during testing.

The test panels were instrumented for the measurement of strain and temperature. Strains were measured using four uniaxial strain gauges that were attached to the inner facesheet of the test panels as indicated in the schematic shown in Fig. 9. Two gauges were located at the center of the panel with one measuring in-plane strain

## Load Introduction Reinforcements



## Inner Facesheet

Fig. 7 X-33 test article.

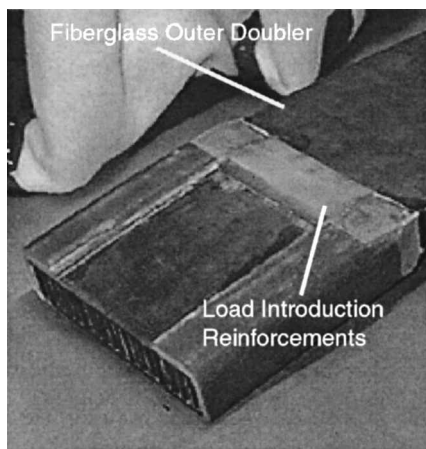


Fig. 8 Specimen preparation details.

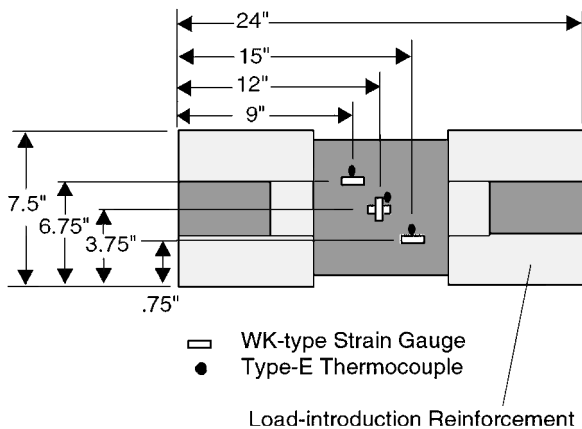


Fig. 9 Test panel instrumentation layout.

in the hoop direction and the other measuring in-plane strain in the transversedirection (refer to Fig. 5). Another gauge was located 3 in. above and 3 in. to the left of center, and the fourth gauge was located 3 in. below and 3 in. to the right of center, with each measuring in-plane strain in the hoop direction (Fig. 9). Temperatures were measured with three type-E thermocouples that were located near each strain gauge location.

### Test Descriptions

Four types of tests were conducted in the present study. In particular, calibration tests, thermal and thermomechanical conditioning tests, liquid-helium leak tests, and liquid-hydrogen leak tests were performed. The calibration tests were used to determine the range

of the leak measurements over which the FMLDS could operate, the accuracy of the FMLDS, and the effect of cryogenic temperatures on the measurements. The thermal and thermal and thermomechanical conditioning tests were performed to ensure that the thermal and mechanical load history of the test panels was as close as possible to those experienced by the actual tank. The liquid-helium leak tests were performed to determine liquid-helium leak rates and to determine measurement techniques before moving on to the final tests, which were used to determine liquid-hydrogen leak rates.

### Calibration Tests

Calibration tests were required to determine the range over which the FMLDS could accurately be used to measure leak rates. The FMLDS was calibrated to determine its accuracy for a range of leakage flow rates and to determine the effects of cryogenic temperatures on the measurements. Two calibration tests were performed: the first to calibrate the flow rates obtained from pressure measurements and the second to determine the overall accuracy of flow measurements made using the FMLDS at both room temperature and cryogenic temperature.

The first calibration test measured the accuracy of the flow-rate measurements obtained from monitoring pressure rises in an evacuated control volume over time, as indicated in the schematic of Fig. 10. Gaseous helium (GHe) was supplied through a standard 50 scc/min flow meter, with an accuracy of 1% of the full scale, across a precision leak valve and into the evacuated control volume where the pressure was measured. Measurements were made at 1, 5, and 40 scc/min by setting the precision leak valve and monitoring the level of flow that registered on the flow meter. For each valve setting the pressure in the evacuated control volume was monitored over a 2-min period, and a flow rate was computed.

The second calibration tests measured the overall accuracy of the FMLDS. This test was designed to measure the errors introduced by the flexible vacuum membrane, the heated seal, and the capillary tubing used to collect leaking gases. These tests were performed at room temperature and at operational cryogenic temperatures to determine if temperature effected the flow measurement. As shown by the schematic of Fig. 11, the FMLDS was attached to the side of a 12 × 12 × 12 in., stainless-steel container that was cooled with liquid nitrogen (LN<sub>2</sub>). GHe was delivered through a precision leak valve to the FMLDS by 0.25-in.-diam stainless-steel tubing and a 0.0625-in.-diam, stainless-steel, capillary tube. The gas was then

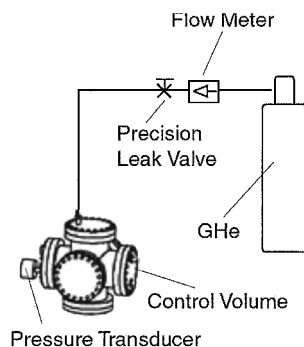


Fig. 10 Flow calibration test setup of the vacuum pressure-measurement system.

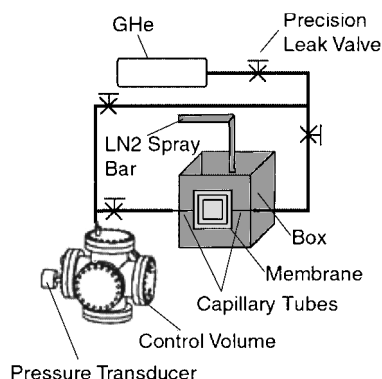


Fig. 11 Test setup for calibration of the FMLDS.

removed from the vacuum membrane through a 0.0625-in. capillary tube passing through the seal material and connected with 0.25-in.-diam stainless-steel tubing to the evacuated control volume, where the pressure and temperature were measured over time. The GHe could also be delivered directly to the control volume by using flow control valves to direct the flow through 0.25-in.-diam stainless-steel tubing, which bypassed the FMLDS. Comparisons of the flow rates measured when gas flowed through this bypass line to flow rates measured when gas flowed through the FMLDS indicated the accuracy of the system at various leak levels, which were controlled through a precision leak valve.

Flow calibration tests were first performed at room temperature, and then the system was used to assess the functionality of the FMLDS seal at cryogenic temperature before flow calibration tests at cryogenic temperatures were performed. When the seal temperature reached approximately 0°F, the seal failed, and pressure in the control volume rose instantaneously to atmospheric pressure. When the inside surface temperature of the stainless-steel container decreased to below -100°F, there was not sufficient heat in the seal-heating loop to maintain the FMLDS seal at 0°F. For the flow tests at cryogenic temperature, the inside surface temperature of the container was maintained above -100°F by controlling the supply of liquid nitrogen to the stainless-steel container through a spray bar. The subsequent FMLDS seal temperature during these tests was 10°F, near the lower limit of the recommended seal operating temperature of 0°F. The flow of heated ethylene glycol was maintained through the seal-heating loop during these tests. Both the room-temperature tests and tests at cryogenic temperature were performed with leak rates varying between 0 and 200 scc/min.

Thermal and Thermomechanical Conditioning

The two test articles were subjected to thermal and thermomechanical conditioning to ensure that thermal and mechanical load history of the test articles was as close to that of the X-33 tank structure as possible. Plots of the temperatures and in-plane mechanical strains that were applied to the test panels during thermal and thermal-mechanical conditioning are shown in Fig. 12, and a photograph of one of the test articles, mounted in the test apparatus prior to conditioning, is shown in Fig. 13. The test panel was placed

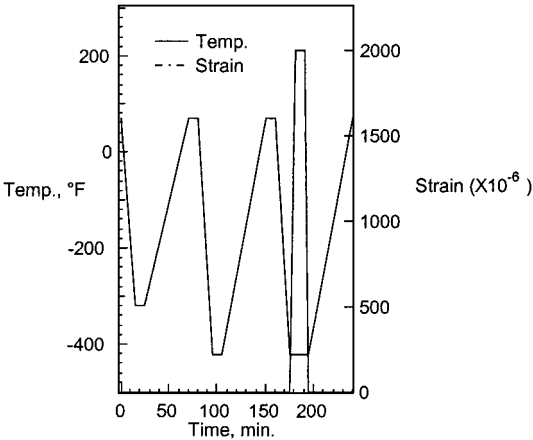


Fig. 12 Thermal and mechanical conditioning profiles for the X-33 panels.

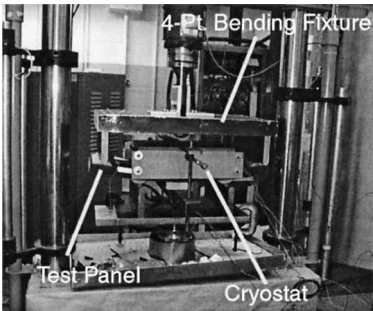


Fig. 13 X-33 panel prior to thermal and thermomechanical conditioning.

in the four-point-bending fixture, and a cryostat (an insulated, five-sided box, with a spray bar used to deliver cryogenic fluid to the test specimen) was then placed on top of the specimen. During conditioning, the temperature was maintained by supplying LN<sub>2</sub> or LHe to the cryostat while load was applied.

Both test panels were thermally cycled first to -320°F by using LN<sub>2</sub>, then to -423°F (LH<sub>2</sub> temperature) by using LHe, and then again to -423°F by using LHe. On the third thermal cycle a mechanical load was applied that resulted in an in-plane tensile strain of 2000  $\mu$ strain in the inner facesheet of the test panel.

Liquid-Helium Leak Tests

After the test panels were conditioned, LHe leak measurements were made in the Thermal Structures Laboratory at NASA Langley Research Center (LaRC). Photographs of the test apparatus are shown in Figs. 14 and 15. The evacuated control volume, the mass spectrometer, the Dewar of liquid helium, and the test article mounted in a 100-kip hydraulic load machine are each visible in Fig. 14. A close-up view of the test specimen, located in the load fixture, is shown in Fig. 15. This figure also shows the stack of compressed foam that was placed beneath the specimen to apply a small positive pressure to the FMLDS seal during testing. Leak measurements were made at inner-facesheet strain values of between 0 and 4000  $\mu$ strain.

Liquid-Hydrogen Leak Tests

Subsequent to the LHe leak tests conducted at NASA LaRC, LH<sub>2</sub> leak measurements were made at the NASA Marshall Space Flight Center's (MSFC) Cold-Flow-Hydrogen Test Facility (CFHTF). These tests were performed at MSFC to determine the leak rate using the actual LH<sub>2</sub> propellant. A photograph of the test setup in a CFHTF test cell is shown in Fig. 16. During LH<sub>2</sub> testing, the panel was sealed in a vented, aluminized Mylar™ bag that captured the hydrogen and vented it safely to the atmosphere. The test hardware (four-point-bending fixture, foam support, and test panel) were then contained within an aluminum chamber, which was purged with GHe during tests (Fig. 17). Leak measurements were made at strain values between 0 and 3750  $\mu$ strain.

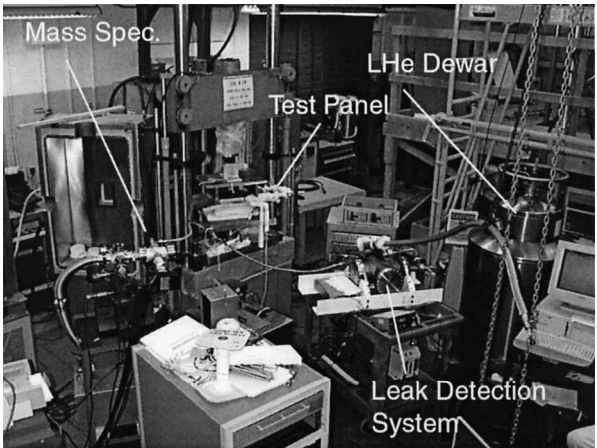


Fig. 14 LHe-leak tests at NASA LaRC.

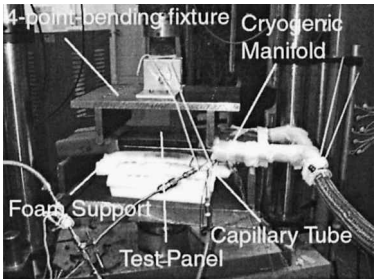
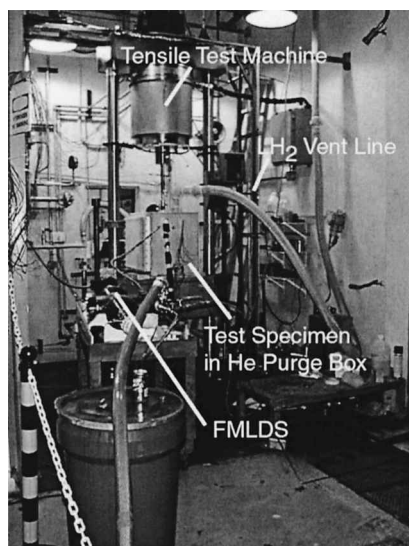
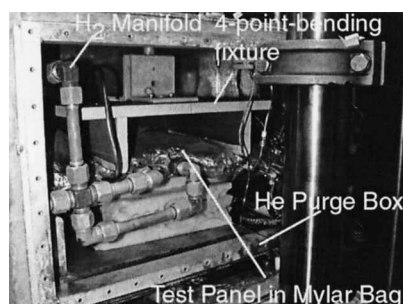


Fig. 15 Close-up of specimen in four-point bend fixture.

Fig. 16 LH<sub>2</sub> test at MSFC.Fig. 17 Close-up of the specimen in the GHe purge box during LH<sub>2</sub> test at MSFC.

## Test Results

### Calibration Test Results

The ratio of the calculated flow rate  $F_m$  to the rate indicated by the flow meter  $F_c$  for the first calibration test is plotted in Fig. 18 as a function of  $F_c$ . As shown, the measured flow rate is accurate to approximately  $\pm 7\%$  at flow rates between 1 and 40 scc/min. For the second calibration test the flow measured through the FMLDS ( $F_m$ ) and through the bypass line ( $F_c$ ) were recorded at each setting of the precision leak valve, and the ratio  $F_m/F_c$  was plotted as a function of  $F_c$  (Fig. 19). Corresponding results from tests at room temperature and at cryogenic temperature are also given in Table 1. At leak levels above 9 scc/min, the error was approximately 2%. For leaks between 0.3 and 9 SCC/min, the error was about 10%.

### Liquid Helium Leak Tests Results

For LHe leak tests of each test panel, measured leak rates were plotted at inner facesheet strains ranging from 0 to 4000  $\mu$ strain in Fig. 20. The leak rate increased with strain until a peak value was reached; that is,  $3.6 \times 10^{-5}$  scc/s-in.<sup>2</sup> at 2000  $\mu$ strain for panel 1 and  $3.6 \times 10^{-4}$  SCC/s-in.<sup>2</sup> at 3250  $\mu$ strain for panel 2. The leak rate then decreased as strain was increased to 4000  $\mu$ strain. These values vary greatly (by an order of magnitude for various strains) between the two test panels.

### Liquid Hydrogen Leak Tests Results

As with the liquid helium tests, the liquid hydrogen leak rates varied widely for each panel tested. For both panels the leak rates varied with strain. For panel 1 the leak rate remained constant at approximately  $5.3 \times 10^{-5}$  scc/s-in.<sup>2</sup>, and it did not begin to increase until the strain in the inner facesheet reached 2500  $\mu$ strain. At this point the leak rate increased as strain increased to a maximum of  $3.7 \times 10^{-2}$  scc/s-in.<sup>2</sup> at 3000  $\mu$ strain. The leak rate then decreased as strain increased to  $3.2 \times 10^{-2}$  scc/s-in.<sup>2</sup> at a maximum strain of 3750  $\mu$ strain. Then, as strain was removed from the inner facesheet

Table 1 Calibration test results

$F_c$ , scc/min	$F_m$ , scc/min	Ratio ( $F_m/F_c$ )
<i>Room temperature data (70°F)</i>		
0.113	0.084	0.75
0.662	0.594	0.90
2.578	2.31	0.90
9.001	8.637	0.96
78.1	76.58	0.98
77.93	76.5	0.98
154.0	154.5	1.00
<i>Cryogenic test data (−100°F)</i>		
0.311	0.277	0.89
24.346	23.861	0.98
206.38	203.346	0.98

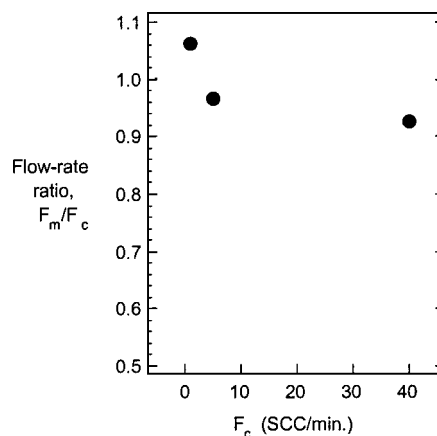


Fig. 18 Flow calibration results for the vacuum pressure-measurement system.

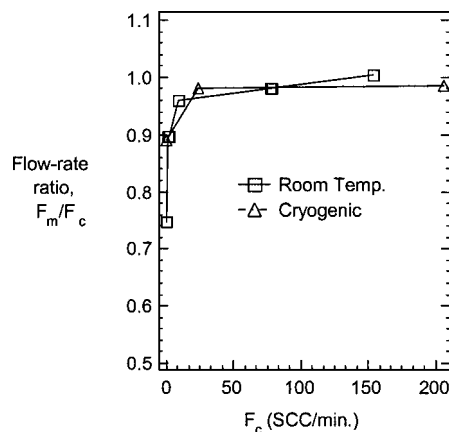


Fig. 19 Test results for calibration of the FMLDS.

the leak rate increased to  $3.4 \times 10^{-2}$  scc/s-in.<sup>2</sup> at 500  $\mu$ strain before falling to  $1.1 \times 10^{-2}$  scc/s-in.<sup>2</sup>, when the load was removed from the panel and the strain in the inner facesheet was zero. This leak rate was substantially higher than the initial leak rate at zero strain ( $5.3 \times 10^{-5}$  scc/s-in.<sup>2</sup>), indicating permanent damage had occurred in the inner facesheet.

The leak rate for panel 2 also increased as inner-facesheet strain increased (peaking at a value of  $2.8 \times 10^{-3}$  scc/s-in.<sup>2</sup> at 3750  $\mu$ strain). Then, as load was removed, the leak rate decreased to  $0.7 \times 10^{-3}$  scc/s-in.<sup>2</sup> with no load applied. This rate was also higher than the initial leak rate of  $0.17 \times 10^{-3}$  scc/s-in.<sup>2</sup> and indicated that permanent damage had occurred in the laminate.

As seen in Figs. 21 and 22, the leak rates for both panels exceed the acceptable leak rate of  $10^{-3}$  scc/s-in.<sup>2</sup> given in Ref. 4. The leak rates for the LH<sub>2</sub> leak tests were an order of magnitude larger than the leak rates for prior LHe tests, which is not explained by the differences in the molecular weight of gaseous He and H<sub>2</sub>.

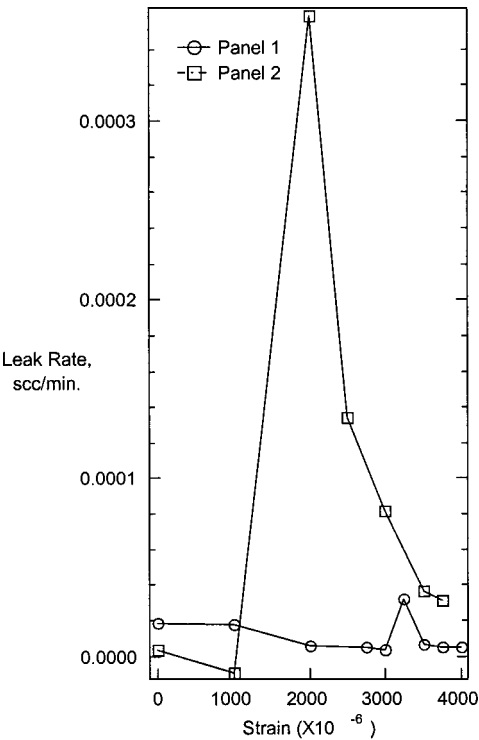


Fig. 20 LHe leak data for panels 1 and 2.

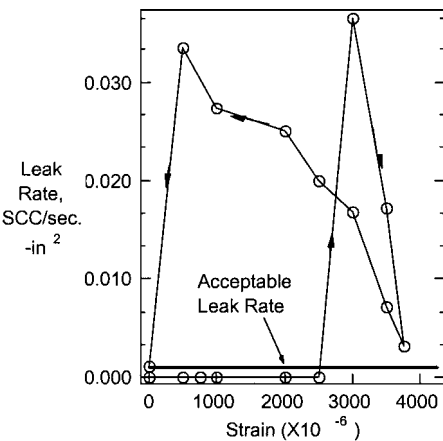


Fig. 21 Panel 1 LH<sub>2</sub> leak data; arrows indicate order in which measurements were taken.

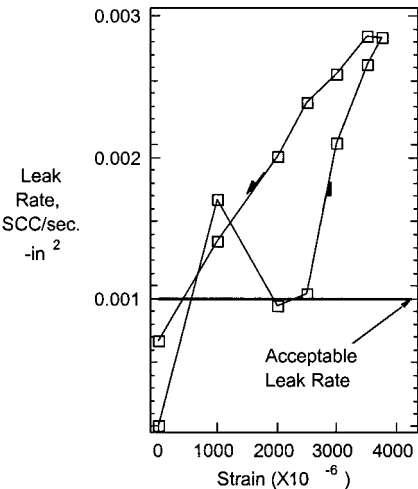


Fig. 22 Panel 2 LH<sub>2</sub> leak data; arrows indicate order in which measurements were taken.

Discussion of Results

The calibration tests indicate that the leak measurement system is capable of measuring leaks between 1 and 200 scc/min with an accuracy of approximately 10%. For the first calibration tests the increase in the error seen at the lowest measured flow rate (1 scc/min) is attributed to the accuracy limitation of the flow meter ( $\pm 0.5$  scc/min). For the second calibration test the results suggest that at leak levels below 1 scc/min (with lower levels of pressure) the conductance through the 0.0625-in. capillary tube limited the flow and increased errors in the measurements, as seen in the data collected.

The measured leak rates indicate a significant leak problem for the X-33 LH<sub>2</sub>-tank inner facesheet. The data gathered for the X-33 tank failure investigation indicate that for the actual structure under thermal and mechanical load, hydrogen leaked at a rate significantly greater than the acceptable leak rate. The apparent leakage was through paths created by interply microcracks that were generated by a combination of ply-level thermal residual stresses and mechanical stresses generated by the internal pressure load. Leak rates varied with the applied load and the test gas used. Also, large variations in leak rates measured for the two panels tested indicate that a wide variation in hydrogen leak rates can be expected (0.0028-0.037 scc/s-in.<sup>2</sup>).

Measured LHe leak rates do not correlate with the corresponding LH<sub>2</sub> leak rates. The lack of correlation could be caused either by accumulated damage in the panels (that is, increases in damage as the panel is repeatedly tested, with additional microcracking resulting in higher leak levels) or leakage by different mechanisms for LHe and LH<sub>2</sub>. This lack of correlation needs further investigation.

Conclusions

An apparatus and method of performing microleak tests that were developed at NASA Langley Research Center (LaRC), in support of the X-33 tank failure investigation, have been presented. Calibration tests that were performed to assess the accuracy of the apparatus across a representative range of leak rates and at cryogenic conditions have been described and discussed. The test method and test apparatus were used to perform leak measurements on a curved, sandwich structure that was subjected to a four-point-bending load at cryogenic temperature. The curved, sandwich structure test specimens consisted of two panels made out of a flawed X-33-LH<sub>2</sub>-tank section. Leak tests of the two test panels were completed, with liquid helium (LHe) leak tests performed at LaRC and LH<sub>2</sub> leak tests performed at NASA Marshall Space Flight Center. The results of these tests have been presented.

The calibration tests conducted indicate that the leak-measurement system is accurate, with less than 10% error for leak rates from 1 scc/min to 200 scc/min. Cryogenic temperatures have no effect on the leak measurements as long as the seal temperature is kept above 0°F. The LHe and LH<sub>2</sub> tests that were conducted indicate that further research is needed to determine whether LHe tests can be used instead of LH<sub>2</sub> tests to determine whether leakage is an issue for various materials when LH<sub>2</sub> leaks are the primary concern. The test results presented herein also indicate that measured LH<sub>2</sub>-leak rates are above acceptable levels that are typically used for a single-stage-to-orbit LH<sub>2</sub> tank and that they can vary widely with load level and location in the structure.

Overall, the investigation presented here has demonstrated the need for structures-level leak testing to validate composites and composite manufacturing processes for LH<sub>2</sub>-tank applications. In addition, a measurement apparatus and method has been presented that can be modified to investigate other loading conditions and geometries. These tests should include thermal and thermal-mechanical conditioning and testing of structures under the actual operational mechanical loads and temperatures.

Acknowledgments

The authors wish to acknowledge Steven J. Scotti from NASA Langley Research Center and Michael C. Watwood and Matthew Jackson from the Illinois Institute of Technology Research Institute for their invaluable contributions to this test program.

## References

- <sup>1</sup>Cook, S., "The X-33 Advanced Technology Demonstrator," AIAA Paper 96-1195, April 1996.
- <sup>2</sup>Dixon, S. C., Tenny, D. R., Rummler, D. R., Weiting, A., and Bader, R. M., "Structures and Materials Technology Issues for Reusable Launch Vehicles," NASA TM-87626, Oct. 1985.
- <sup>3</sup>McCarty, R. D., Hord, J., and Roder, H. M., "Selected Properties of Hydrogen (Engineering Design Data)," National Bureau of Standards, Monograph 168, Boulder, CO, 1981.
- <sup>4</sup>Robinson, M. J., "Composite Cryogenic Propellant Tank Development," *Proceedings of the AIAA/ASME/ASCE/AHS/ASC 35th Structures, Structural Dynamics, and Materials Conference*, Vol. 1, AIAA, Washington, DC, 1994, pp. 544–551.
- <sup>5</sup>"Final Report of the X-33 Failure Investigation Team," *X-33: Reusable Launch Vehicle—Space Transportation* [online database], URL:

<http://x33.msfc.nasa.gov> [cited 24 Jan. 2001.]

- <sup>6</sup>Kumazawa, H., Aoki, T., Ishikawa, T., and Susiki, I., "Modeling of Propellant Leakage Through Matrix Cracks in Composite Laminates," AIAA Paper 2001-1217, April 2001.
- <sup>7</sup>Jones, R. M., *Mechanics of Composite Materials*, Taylor and Francis, Washington, DC, 1975, pp. 147–156.
- <sup>8</sup>"Standard Test Method for Determining Gas Permeability Characteristics of Plastic Film and Sheeting," American Society for Testing and Materials, ASTM-D 1434-82, 1998.
- <sup>9</sup>Halliday, D., and Resnick, R., "Ideal Gas—A Macroscopic Description," *Fundamentals of Physics*, 2nd ed., Wiley, New York, 1986, pp. 408, 409.

M. P. Nemeth  
Associate Editor